



Effect of hydration on microstructure and property of anodized oxide film for aluminum electrolytic capacitor

Chao-Lei Ban¹ · Fang-Ren Wang¹ · Jian-Hai Chen¹ · Zhen-Qi Liu¹

Received: 29 May 2018 / Accepted: 18 July 2018 / Published online: 20 July 2018
© Springer Science+Business Media, LLC, part of Springer Nature 2018

Abstract

Etched aluminum foil for aluminum electrolytic capacitor was first boiled in water for different time to form hydrous film on Al foil and then anodized in H_3BO_4 solution at 530 V to form anodic oxide barrier film as insulating dielectric layer. The obtained films were characterized by field-emission scanning electron microscopy, transmission electron microscope and X-ray diffraction for surface morphology, microstructure and crystallinity examination. Small-current charging, LCR meter and electrochemical impedance spectroscopy were exploited to measure the properties of the anodized oxide film such as withstanding voltage (U_w), specific resistance (R_{ox}) and specific capacitance (C_s and C_{ox}) for its electrochemical performance. The results show that the hydrous film is pseudoboehmite (PB) with a dense inner layer and a fibrous outer layer. The crystallinity of the PB film increases with hydration time. During anodization, the PB film was transformed into anodic oxide (γ' - Al_2O_3) barrier film. Prolonging hydration time promotes transforming PB into γ' - Al_2O_3 and improves the crystallinity of the barrier film, leading to increase in C_s and C_{ox} and decrease in R_{ox} and U_w .

1 Introduction

Aluminum electrolytic capacitors are extensively used in the electronic industry. Despite their use for several decades, research and development efforts to improve the performance of the capacitor are still underway [1–4]. The capacitor consists of an anode foil on which an oxide is formed appropriate to the voltage required for operation, a suitable electrolyte and a cathode foil. A high capacitance device requires a high surface area coated with a suitable dielectric material. For aluminum electrolytic capacitors, the high surface area is obtained by electrochemical etching and subsequent tunnel-widening. The dielectric film is grown directly on this surface by anodization. The oxide thickness obtained in formation is proportional to the voltage used for the oxide during anodizing [5–7].

Among the components of the aluminum electrolytic capacitor, the barrier aluminum anodized oxide film plays the crucial role during operation. The barrier aluminum anodized oxide film can be amorphous or crystalline from different anodizing conditions. Comparing the amorphous

oxide film, the crystalline one is characteristic of lower ionic conductivity and high relative dielectric constant and high voltage sustaining. Developing the crystalline oxide film has a continuous attraction for researchers [8–10]. Crystalline oxide growth may be promoted by the presence of a thin layer of thermal oxide on the surface of aluminum [11], anion species of electrolytes [12, 13], and high formation voltage [14], etc.

Another popular way to make a crystalline anodic oxide is to react the Al substrate with boiling water to deposit a hydrous oxide, and then to anodize in a neutral borate solution at high temperature [15, 16]. This process has been of technological importance for some time in the manufacture of electrolytic capacitors but has received scant attention in the scientific literature. Therefore, a more detailed knowledge of the structure of the hydrous oxide as formed, its growth sequence, and transformation to the crystalline dense barrier layer is required. To meet the more severe performance requirements that are being placed on electrolytic capacitors, oxide dielectrics with enhanced long-term stability are also needed. To achieve this, we need more detailed knowledge of the anodic oxide film. This present paper presents the characterization of these films and new features of the oxide structure and growth process are revealed. The effect of hydration on the performance and microstructure of the barrier aluminum anodized oxide film is studied.

✉ Chao-Lei Ban
banchaolei@163.com

¹ School of Materials Science and Engineering, Liaocheng University, Liaocheng 252059, China

2 Experimental details

2.1 Specimen and films preparation

Commercially tunnel-etched 99.99% pure aluminum foil with 95% {100} <100> cubic texture was used throughout. Tunnels mainly develop along <100> direction normal to the surface. The tunnels are about 1–2 μm wide and 25–30 μm long averagely. The tunnel density is about 10^7 cm^{-2} .

2.2 Hydrous and anodized oxide films preparation

The hydrous oxide films were deposited on 10 cm^2 Al foil coupons by reaction of the substrate with neutral boiling DI-water followed by a drying step in air at room temperature for 15 min. The reaction times ranged from 5 min up to 25 min.

For anodized oxide film preparation, the above hydrated foil coupons is subjected to primary anodization in 1.29 M H_3BO_4 solution at 95 °C, heat-treatment at 500 °C for 2 min followed by reanodization in the same solution. During primary anodization and reanodization, the cd was held at 25 mA cm^{-2} until the cell voltage increased to a value $V_f=530 \text{ V}$ and then V_f was maintained for 20 and 5 min, respectively.

2.3 Microstructure characterization

A high power X-ray diffractometer (MAC Science Co. Ltd M21X) was adopted to determine the crystallographic structure of the hydrated or anodic films on Al substrate. 2-theta scans were performed on a 2θ range of 10° – 90° . The samples were measured in a continuous mode with 0.02° step size and a scan speed of $10^\circ \text{ min}^{-1}$.

The surface and cross sections of the grown films on Al foil substrate were examined with a field emission scanning electron microscope (FE-SEM) and a transmission electron microscope (TEM, Hitachi H-800H), respectively. An electron beam with 1.5 keV acceleration voltage and 20 μA current was used for surface imaging. All films were carbon-sputtered prior to the FE-SEM analysis. For cross-section microstructure analysis, the hydrated or anodized foils were thinned with a focused beam of Ar ions radiating parallel to the plane of the specimen face to a proper thickness. During TEM observation, a camera length of 80 cm was adopted during the nanobeam electron diffraction operating at 175 kV.

2.4 Performance and property

Electrochemical workstation and three-electrodes tests were carried out to measure the electrochemical performances of the anodic aluminum films in 30 °C 0.4 M $\text{NH}_4\text{B}_5\text{O}_8 \cdot 4\text{H}_2\text{O}$ electrolyte. The working electrode, counter one and reference one are the anodized foil, a platinum sheet and a

saturated calomel electrode, respectively. The reference electrode was almost connected to the working electrode by a salt bridge with a probe. An EG&G model 273A potentiostat connected to a Schlumberger 1255 frequency response analyzer was employed to make electrochemical impedance spectroscopy (EIS). The samples were measured from 100 kHz to 10 mHz, with a 10 mV root mean square amplitude at the open circuit potential.

A pure aluminum sheet with a very large area and a LCR meter were adopted to measure the specific capacitance of the anodized foils in 30 °C 0.4 M $\text{NH}_4\text{B}_5\text{O}_8 \cdot 4\text{H}_2\text{O}$ electrolyte. For withstanding voltage measurement, the anodized foils were charged with $cd=0.2 \text{ mA cm}^{-2}$ for 800 s in 80 °C 0.9 M H_3BO_4 solution. For withstanding voltage (U_w) measurement, the cell voltage (E_c) with time curves (E_c vs. t) were recorded and monitored by a digital multi-meter connected to a PC system.

3 Results and discussion

3.1 FE-SEM and TEM of hydrous and anodized oxide films

A micrograph of the Al substrate used for hydrous oxide film growth is presented in Fig. 1a. One to two micrometers radius tunnels along <100> directions can be observed in the Al substrate as a result of electrochemical etching and subsequent widening. Figure 1b–f show FE-SEM micrographs of the hydrous oxide films formed by reactions of the substrate with boiling DI water for 5, 10, 15, 20 and 25 min respectively. Fine corn-flakes structures with 20–70 nm-size petals are formed upon immersion in boiling water for 5 min. With increasing hydration time, cotton-ball structures gradually took place of corn-flakes ones. But a few corn-flakes structure observed for early times (5 min) was nicely still preserved even in very long hydration samples (20 min). Finally, the hydrous oxide film formed on Al substrate continued to grow even further with hydration time forming a dense layer (25 min). Some narrow fine tunnels were clogged by excess hydrous oxide with hydration time.

Figure 2a–e show FE-SEM micrographs of the anodized oxide film following hydration in boiling water for 5, 10, 15, 15 and 20 min respectively. The corn-flakes and cotton-ball structure observed for hydrous oxide film have been disappeared, replaced by the barrier anodic oxide film. It seems that long hydration time increases the risk of blockage for tunnels by anodic oxide film, resulting in decreasing the available surface area by etching and specific capacitance of anode foil.

Figure 3a, b shows TEM micrographs of cross-section for hydrous oxide film in etch tunnel from 10 min reaction with boiling water and its corresponding anodized oxide

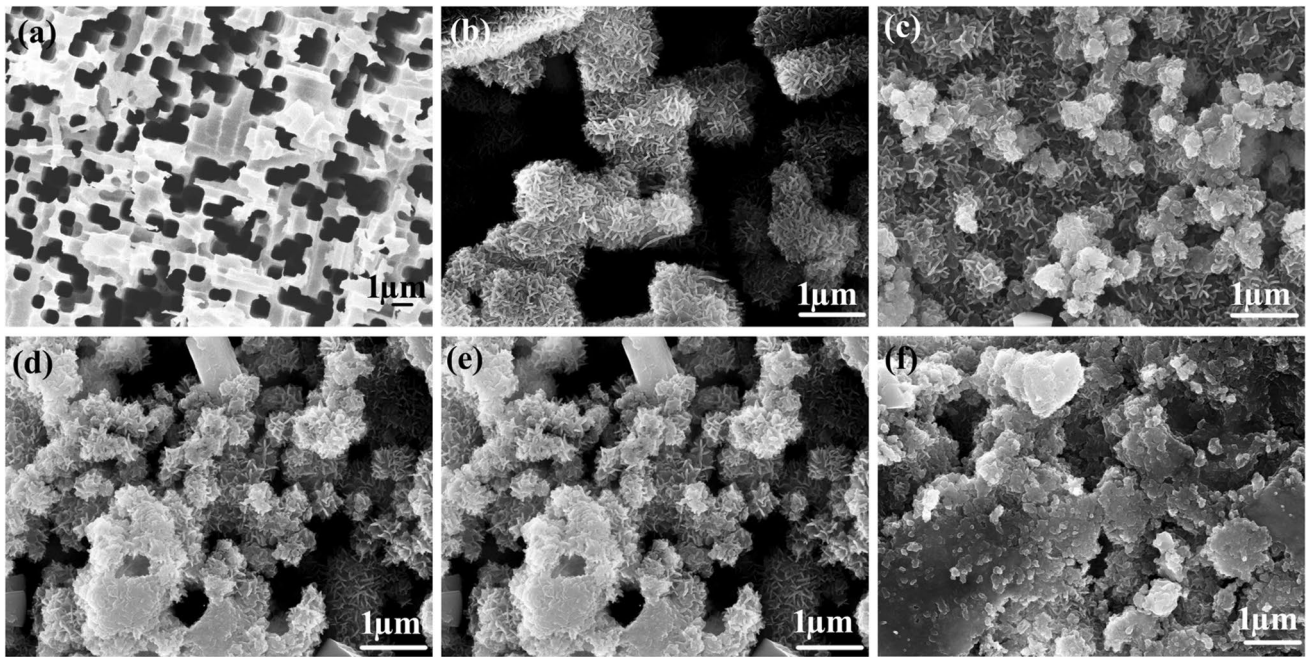


Fig. 1 FE-SEM micrographs of **a** the tunneled Al foil and hydrous oxide films by hydration in boiling water for **b** 5 min, **c** 10 min, **d** 15 min, **e** 20 min, **f** 25 min

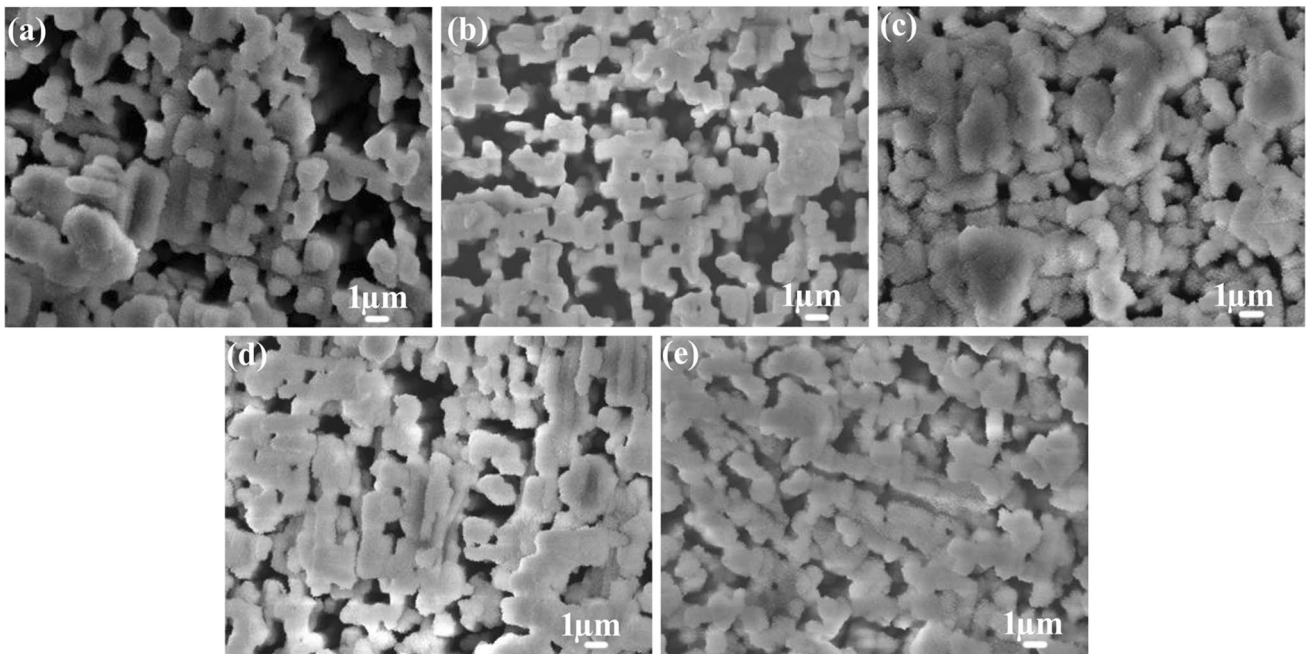
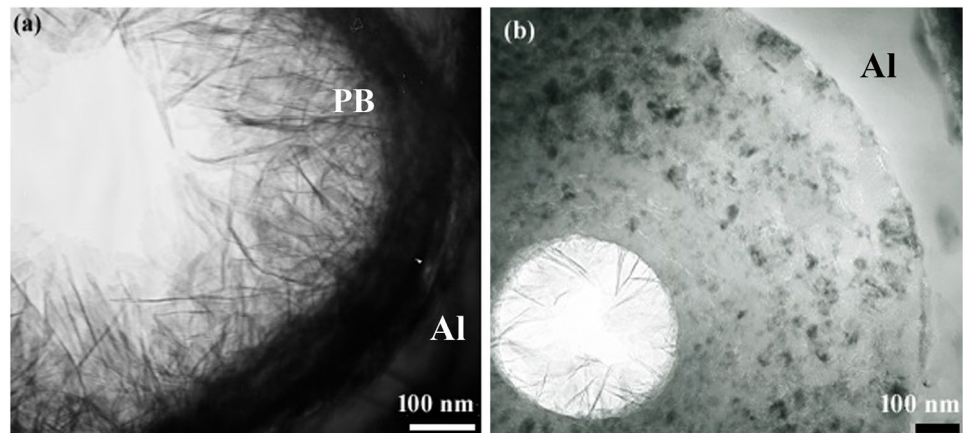


Fig. 2 FE-SEM micrographs of anodized oxide film following hydration in boiling water for **a** 5 min, **b** 10 min, **c** 15 min, **d** 20 min, **e** 25 min

film, respectively. The considerable structural details of both films are further revealed. The hydrous oxide film has a dense inner layer 100 ± 20 nm thick and a fibrous outer layer ~ 200 nm thick that is embedded in epoxy resin. It is difficult to get a precise measure of the dense layer thickness because

of the uncertainty in the position of the dense/fibrous interface. The fibers are as thin as about 0.8 nm. The hydrous oxide film has a structure of opposing sheets of Al–O octahedra joined by a channel of hydrogen bonds. The unit cell thickness in the direction normal to the H-bond channel is

Fig. 3 TEM micrographs of **a** hydrous oxide films in etch tunnel from 10 min reaction with boiling water and **b** its corresponding anodized oxide film



reported to be about 0.68 nm but this can be increased by water incorporated into the H-bond channel. The thinnest fibers are likely to consist of two H-bonded sheets. The white gap at the metal/hydrous oxide film interface develops during TEM observation due to evaporation of H_2O from the hydrous oxide film, especially when examining at high magnification.

The barrier anodized oxide is about 550 nm thick and consists of a darker inner zone and a lighter outer zone of about equal thickness. It has been reported that the inner layer is from crystallization of amorphous anodic oxide and the outer layer is from the hydrous oxide film transformation. The dense region for hydrous oxide film has disappeared but residual fibrillar region for hydrous oxide are still seen at this voltage anodized oxide film. Small dark regions are scattered throughout the barrier layer. A network of fine circular cracks, about 2 wide, is seen in this specimen. The cracks seem most numerous in the outer half of the barrier layer but do not extend to the hydrous oxide interface. These cracks may also be an artifact of the sample preparation for TEM observation, as well as due to phase transformation from hydrous oxide to anodized one and resulted shrinkage.

3.2 XRD of hydrous and anodized oxide films

Analysis of X-ray diffraction (XRD) patterns of films prepared by hydration of Al substrate for different time, identified these films as orthorhombic pseudo-boehmite (PSB), as seen in Fig. 4. This material is a poorly crystallized boehmite (BOE) with a water content of 1.5–2.5 mol. BOE and PSB have the same crystalline structure but different crystalline dimensions. The existence of this PSB structure was proven previously by Geiculescu and Strange [17]. Figure 4 shows that the hydrous oxide PSB film formed on Al substrate continued to grow even further with hydration time, forming a dense, highly crystalline layer, in consistent with Fig. 1 observation.

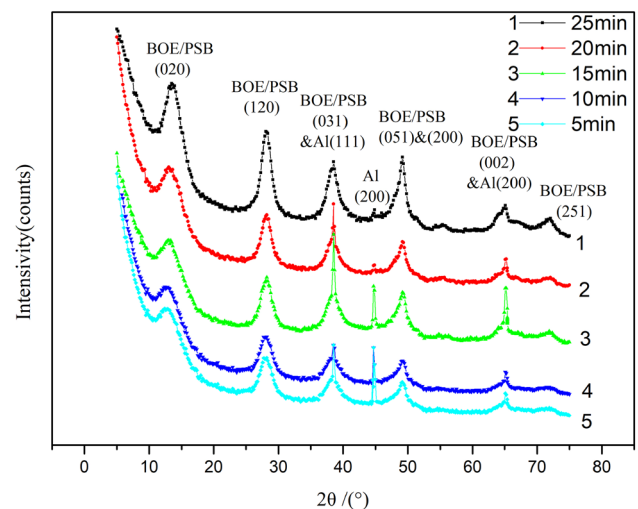


Fig. 4 XRD patterns of the hydrous oxide films on tunnel-etched Al foil prepared by hydration in boiling water for (5) 5 min, (4) 10 min, (3) 15 min, (2) 20 min, (1) 25 min

Figure 5 shows XRDs of the anodized Al foils following hydration in boiling water for different time. Figure 5 indicates that the strongest peak corresponds to Al (200) and other distinct peaks comes from crystalline oxide in barrier films, marked by γ' - Al_2O_3 (440) and γ' - Al_2O_3 (400). γ' - Al_2O_3 is a defect spinel similar to γ - Al_2O_3 but with more disorder on the cation lattice. The γ' - Al_2O_3 (440) peaks can be used to analyze the crystallinity of the anodic oxide films with the Scherrer formula $d = k\lambda / (B \cdot \cos\theta)$, where d is the crystallite size, k is a form factor, $k = 0.89$ for spheres particles, λ is the wavelength of the radiation used, $\lambda_{Cu, K\alpha 1} = 1.54056 \text{ \AA}$, B is half height width of the peaks. The crystallite size increased with hydration time, indicating improvement of the crystallinity.

As Fig. 4 shows, the hydrous oxide is PSB, an oxyhydroxide containing excess water with approximate composition $AlOOH \cdot H_2O$. The PSB is not a significant barrier to ion

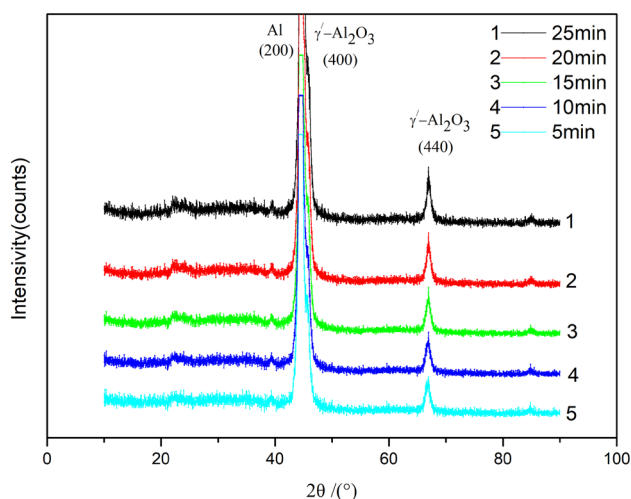


Fig. 5 XRD patterns of the anodized oxide films on tunnel-etched Al foil following hydration in boiling water for (5) 5 min, (4) 10 min, (3) 15 min, (2) 20 min, (1) 25 min

or water transport and has a low density of 2.47 g cm^{-3} . During anodization, Al^{3+} cations move to the PSB interface under electric field, where they take part in the transformation of PSB to γ' - Al_2O_3 . A proposed reaction is $\text{AlOOH}\cdot\text{H}_2\text{O} + \text{Al}^{3+} \rightarrow \gamma'\text{-Al}_2\text{O}_3 + 3\text{H}^+$. By anion transport to the metal interface, amorphous alumina grows under the PSB layer. Crystallites from the PSB transformation serve as seeds for transformation of the amorphous anodic oxide to γ' - Al_2O_3 . Figure 5 suggests that the different time-formed PSB films have been completely transformed into anodic γ' - Al_2O_3 films during anodization, because there isn't obvious diffraction peaks for PSB, as shown by Fig. 4. Maybe, some PSB still survives, as shown by Fig. 3b. However, their amount is too small to be refracted by XRD.

3.3 Effect of hydration on electrochemical property of anodized oxide film

The results of EIS measurements (Nyquist plots) for the anodized Al foil following hydration in boiling water for different time are given in Fig. 6. Over the frequency range in the investigation, a single time-constant capacitance behavior is predominant, characteristic of a dielectric material. An equivalent electrical circuit model inset in Fig. 6 was used to interpret the Nyquist plots. The equivalent electrical circuit consists of a specific capacitance (C_{ox}) of the anodized oxide film, a specific resistance (R_{ox}) of the anodized oxide film and a solution resistance (R_s). By fitting the obtained impedance data with the equivalent circuit, the circuit parameters, such as R_{ox} and C_{ox} , were approximately evaluated and given in Table 1. Here, C_{ox} and R_{ox} were nominal values, ignoring the effect of the etched foils area. In Table 1, the film's withstanding voltage (U_w) and specific capacitance

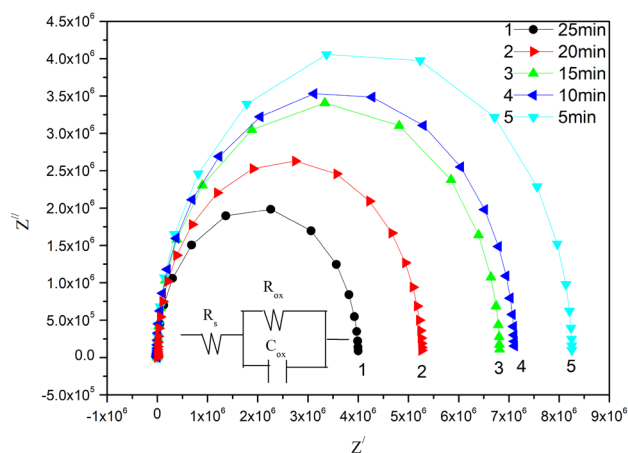


Fig. 6 Electrochemical impedance spectra (Nyquist plot) for anodized foils following hydration in boiling water for different time

(C_s), which are measured with small-current charging and LCR meter, respectively, are also listed. It can be found that the film's specific capacitance (C_s) measured with LCR is almost equal to its C_{ox} stimulated from Nyquist plots. Comparing the amorphous barrier aluminum oxide film, the crystalline one possesses high field strength (E) and high dielectric constant (ϵ_r). Usually, the film thickness (d) can be expressed by $d = V_f \times E$, where V_f is the formation voltage during anodization. As a result, the crystalline anodic oxide film becomes thinner than amorphous one under the same V_f , which can reduce the trend for anodic film to block off fine etch tunnels and increase the Al foil's actual surface area after anodization.

According to the equation $C = \epsilon_0 \epsilon_r A / d$, where ϵ_0 is dielectric constant in vacuum, ϵ_r the relative dielectric constant of the anodic film, A is the actual area of Al foil's actual surface area after anodization, when the anodic oxide film becomes more crystallized with increasing hydration time under the same V_f , ϵ_r and A increase but d decreases, leading to improvement of C_{ox} . However, R_{ox} and U_w decreased with prolonging hydration time. The transformation of pseudo-boehmite (PB) to more dense oxide under electric field result in shrinkage that causes high tensile stress and leaves

Table 1 R_{ox} , C_{ox} , C_s and U_w of anodized oxide films with different time hydration

Film types (min)	R_{ox} ($\text{M}\Omega \text{ cm}^{-2}$)	C_{ox} ($\mu\text{F cm}^{-2}$)	U_w (V)	C_s ($\mu\text{F cm}^{-2}$)
5	9.366	0.5713	533.7	0.5726
10	8.538	0.5972	532.6	0.5958
15	7.904	0.6268	531.8	0.6277
20	7.158	0.6537	531.2	0.6516
25	6.629	0.6702	530.6	0.6784

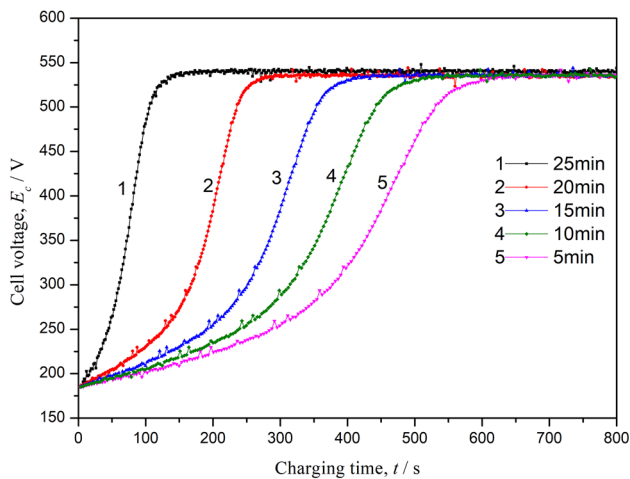


Fig. 7 E_c - t curves of anodic oxide films with different time hydration during charging with small current

microscopic voids buried within the anodic oxide film. The longer the hydration, the more crystallized of the film and the more cracks and microscopic voids, leading to lower R_{ox} and U_w .

Figure 7 shows E_c - t curves of anodic oxide films with different time hydration during charging with small current. It can be found that with hydration time increasing, the E_c - t curves become flat in the slope and reach a low plateau voltage, namely, the withstand voltage (U_w). The charging current is probably used to repair and fill the structural defects such as cracks and microscopic voids of the anodic film by forming new oxide. With hydration time increasing, the anodic film is rich in structural defects ascribing from transformation of PB film to γ' - Al_2O_3 , leading to induction in E_c - t slope and U_w .

4 Conclusion

Prior to anodization in boric acid solution, aluminum capacitor foil with a tunnel etch structure for high voltage electrolytic capacitors is hydrated in boiling water for different time. The effects of hydration on the microstructure, capacitance and resistance of anodized aluminum foils are experimentally investigated here and the important results can be summarized.

1. Prolonging hydration time in boring water helps to prepare crystalline hydrous oxide films on a high purity etched Al foil substrate.

2. During anodization, the PB film was transformed to crystalline anodic oxide layer. The crystallinity of the anodic oxide film is improved with hydration time and increase C_s of the barrier film.
3. Transformation of PB film to γ' - Al_2O_3 is accompanied by void and cracks formation, leading to decrease in U_w and R_{ox} of the barrier film.

Acknowledgements The work is financially supported by the Natural Science Foundation of Shandong Province, China (Grant No. ZR2017MEM019), Technology and Culture Innovation Fund for Student of Liaocheng Univerisy (Grant No. 26312171923) and Innovative Entrepreneurship training Program for College students of Liaocheng Univerisy (Grant No. 201710447009).

References

1. Z.S. Feng, J.J. Chen, C. Zhang, N. Zhao, Z. Liang, *Ceram. Int.* **38**, 2501 (2012)
2. Z.H. Hou, J.H. Zeng, J.J. Chen, S.J. Liao, *Mater. Chem. Phys.* **123**, 625 (2010)
3. K. Watanabe, M. Sakairi, H. Takahashi, S. Hirai, S. Yamaguchi, *J. Electroanal. Chem.* **473**, 250 (1999)
4. C.L. Ban, S.Q. Zhu, J.L. Hou, F.R. Wang, J. Wang, Z.F. Jia, J.S. Zhao, *J. Mater. Sci. Mater. Electron.* **28**, 10992 (2017)
5. J.K. Chang, C.M. Liao, C.H. Chen, W.T. Tsai, *J. Power Sources* **138**, 301 (2004)
6. K. Watanabe, M. Sakairi, H. Takahashi, K. Takahiro, S. Nagata, S. Hirai, *J. Electrochem. Soc.* **148**, 473 (2001)
7. C.L. Ban, S.Q. Zhu, J.L. Hou, F.R. Wang, J. Wang, *J. Mater. Sci. Mater. Electron.* **28**, 6860 (2017)
8. G.A. Hutchins, C.T. Chen, *J. Electrochem. Soc.* **133**, 1332 (1986)
9. P.G. Anderson, O.F. Devereux, *J. Electrochem. Soc.* **122**, 267 (1975)
10. T.A. Libsch, O.F. Devereux, *J. Electrochem. Soc.* **122**, 1654 (1975)
11. J.K. Chang, C.M. Lin, C.M. Liao, C.H. Chen, W.T. Tsai, *J. Electrochem. Soc.* **151**, 188 (2004)
12. C.L. Ban, Y.D. He, X. Shao, J. Du, *Trans. Nonferrous Met. Soc.* **23**, 1039 (2013)
13. C.L. Ban, Y.D. He, X. Shao, *J. Mater. Sci. Mater. Electron.* **24**, 3442 (2013)
14. H.J. Oh, J.H. Lee, H.J. Ahn, Y.S. Jeong, C.H. Heo, C.S. Chi, *J. Electroceram.* **17**, 369 (2006)
15. J.H. Lee, K.W. Jang, H.J. Oh, *Mater. Sci. Eng. A* **449–451**, 314 (2007)
16. H. Uchi, T. Kanno, R.S. Alwitt, *J. Electrochem. Soc.* **148**, 17 (2001)
17. A.C. Geiculescu, T.F. Strange, *Thin Solid Films* **426**, 160 (2003)